

# Short-term adsorption of gold using self-flocculating microalga from wastewater and its regeneration potential by bio-flocculation

Na Shen\*, E.M.N. Chirwa

University of Pretoria, Department of Chemical Engineering, Lynnwood Road, Private bag X20 Hatfield, Pretoria 0002, South Africa.

## Abstract

The challenge of economical separation of tiny microalgal cells from diluted solutions restricts their industry commercialization as promising biosorbents. In this study, freshwater self-flocculating microalga *Tetradesmus obliquus AS-6-1* was used as biosorbent to recover gold from wastewater. Maximum Au(III) adsorption capacity were obtained at optimal conditions of 0.1 g L<sup>-1</sup> biomass, pH 2.0, 25 °C within 30 min for an initial concentration of 5 mg L<sup>-1</sup>. The higher maximum adsorption capacity ( $q_m$ ) and Langmuir constant (b) for *T. obliquus AS-6-1* indicated its potential as efficient adsorbent for gold recovery. Detailed surface characterization demonstrated that polysaccharides excreted from the self-flocculating microalga were responsible for the better adsorption performance of *T. obliquus AS-6-1*. Flocculating activity results showed that *T. obliquus AS-6-1* could efficiently settle down at the bottom by bio-flocculation within 20 min. The regenerated microalgae in the funnel reactor retained high adsorption efficiency of > 97 % in the first two adsorption/desorption cycles. The results from this study firstly demonstrated that the self-flocculating microalga not only benefited its biomass recovery by its bio-flocculating property, but also improved its potential for gold recovery from wastewater.

**Keywords:** self-flocculating microalga; biosorption; gold recovery; bio-flocculation; regeneration

## Introduction

Recovery of gold from the secondary sources such as electronic equipment and electroplating wastewater has been a focus research in recent years (Syed et al. 2012). Various methods have been used for gold recovery, including chemical precipitation, ion exchange, electrochemical methods and membrane processes. However, those

processes suffer from high capital costs and generation of large quantities of secondary wastes, especially in the processing of practical metal wastewater containing precious metals at concentrations below 10 - 40 mg L<sup>-1</sup> (Umeda et al. 2011).

Biosorption, a metabolism-independent process, has been proposed as a potentially attractive and environmentally friendly alternative to physical-chemical processes for the recovery of precious metals from aqueous solutions (Volesky 2007; Mack et al. 2007). Bacteria (Deplanche and Macaskie 2008), fungi (Nakajima 2003), yeast (Lin et al. 2005), algae (Ju et al. 2016), agro wastes (Maruyama et al. 2014) and biopolymers (Gao et al. 2017) have been tested as potential adsorbents in the process of biosorption. Certain microalgae species recently attracted attention due to their unique surface properties which show binding affinity for divalent metals in general and, in some species, precious and rare earth metals particularly. However, due to their small size (2-20 µm) and strong negative charge on cell surface, the economical harvesting/separation of microalga cells from large volume solutions poses a formidable challenge for their industry commercialization (Shen et al. 2017). The immobilization of microalgae could be a great solution to solve this problem, but the mass transfer limitation and additional process cost restrict their practical application (Moreno-Garrido 2008).

Bio-flocculation is considered as the most efficient, economical and technologically feasible method to harvest/separate microalgae from diluted solutions (Zhou et al. 2015). Recently, several self-flocculating microalgae, such as *E. texensis* SAG79.80, *T. obliquus* AS-6-1 and *C. vulgaris* JSC-7 have demonstrated their bio-flocculating properties (Alam et al. 2015; Zhang et al. 2016), with the ability to aggregate together and form flocs, which facilitate their gravity sedimentation for separation from aqueous solutions. In addition, there is no need of additional chemical agents in the separation process of self-flocculating microalgae from diluted solutions (Zhang et al. 2016). Compared with the commonly used separation methods, such as centrifugation and filtration, the use of bio-flocculation is expected to be energy-saving, environmentally-friendly and cost-effective in large-scale microalga application. However, to the best of our knowledge there is no report assessing detailed studies on short-term adsorption of gold using the self-flocculating microalgae and its regeneration potential by bio-flocculation in adsorption/desorption cycles.

In this study, *T. obliquus AS-6-1*, a freshwater self-flocculating microalga was selected as a biosorbent to adsorb Au(III) from wastewater. The Au(III) adsorption performed by *T. obliquus AS-6-1* was examined under different conditions while the non-flocculating microalga *Tetradismus obliquus* used as a control. Kinetics, equilibrium, thermodynamics, surface characteristics and flocculation activity test of biosorbents were carried out. The aim of this study was to investigate the feasibility of self-flocculating microalga *T. obliquus AS-6-1* as biosorbent for short-term adsorption of gold. The consecutive adsorption/desorption cycles in the funnel reactor were investigated to determine the possibility of regeneration of algal biosorbent using its self-flocculating property. The study provides new insights for gold recovery using the self-flocculating microalga and its regeneration potential by bio-flocculation.

## **Materials and methods**

### **Preparation of adsorbent and chemicals**

The self-flocculating microalga *T. obliquus AS-6-1* was initially isolated from freshwater located in southern Taiwan (Zhang et al. 2016). The non-flocculating strain *T. obliquus* (CCAP No. 276/7) was purchased from the Culture Collection of Algae and Protozoa (CCAP) for comparison purpose. These pure strains were cultured in a 12 L culture vessel containing 10L of Blue-Green (BG11) medium (Chen et al. 2016) under algal light conditions (Osram L 36 W/77 Floura) at  $25\pm 1$  °C. The strains were then harvested from the growth media after 15 days and washed thoroughly with deionized water before freeze-drying.

A standard stock solution of  $1000 \text{ mg L}^{-1}$  of chloroauric acid ( $\text{HAuCl}_4$ ) was used to prepare initial Au(III) concentrations between 5 and  $50 \text{ mg L}^{-1}$ . The pH of the metal solution was adjusted with 0.1 M NaOH/ 0.1M HCl. Thiourea was used as eluent for Au desorption from biomass. All the reagents were of analytical grade and procured from Sigma–Aldrich.

### **Optimization of parameters in batch adsorption**

The lyophilized *T. obliquus AS-6-1* and *T. obliquus* were used as adsorbents in batch. All experiments in this study were replicated to ensure consistency and reproducibility of the results. The error bars represent the mean's standard deviations of the triplicates.

Different biomass dosages (0.02 - 0.12 g L<sup>-1</sup>) were used as biosorbents in 100 mL of Au(III) solution with an initial concentration of 5 mg L<sup>-1</sup>. The flasks were then shaken for 480 min at 25 °C. Samples were taken at predetermined time intervals, centrifuged and the filtrate was analyzed using Atomic Absorption Spectrometer (AAS Perkin Elmer AAnalyst 400). Effect of pH was conducted in 100 mL of 5 mg L<sup>-1</sup> of Au(III) solution with varying pH from 1.0 to 7.0. Effect of temperature on biosorption was studied at different temperatures (7, 25, 30, 40, 50 and 60 °C). Batch adsorption studies were carried out at optimized adsorption parameters with initial Au(III) concentrations in the range of 5-50 mg L<sup>-1</sup> to determine the variation in adsorption capacity and efficiency.

### **Adsorption isotherm, kinetics and thermodynamics**

The adsorption equilibrium data obtained at the optimized conditions were modeled using Langmuir (1918) and Freundlich (1906) isotherms to identify the species with the highest adsorption capacity preceding any further biosorption studies. In this study, the Pseudo first-order and Pseudo-second-order (Ho and Mckay 2000) models were applied to analyze the rate of adsorption uptake. The model with the highest correlation coefficient value ( $R^2$ ), close to unity was considered the best fit. Thermodynamic parameters like the changes in standard free energy ( $\Delta G^0$ ), standard enthalpy ( $\Delta H^0$ ) and standard entropy ( $\Delta S^0$ ) were calculated for the evaluation of feasibility of the adsorption reaction (Al-Saidi 2016) (Details of isotherm, kinetics and thermodynamics provided with supplementary material).

### **Characterization of biosorbent**

The elemental composition on the surface of *T. obliquus* AS-6-1 samples before and after adsorption was analyzed by X-ray fluorescence (XRF) spectrometry. Fourier transform infrared spectroscopy (FTIR-Nicolet iS5, Thermo, South Africa) was analyzed to find out the functional groups of adsorbent for Au(III) adsorption. The surface morphology of the tested algae was observed by a scanning electron microscopy (SEM, JOEL JSM 5800LV, Tokyo, Japan). Flocculation activity tests were performed as the same procedures conducted by Guo et al. (2013) (The detailed methodology provided with supplementary material).

## Regeneration of biosorbent

In order to test the regeneration potential of microalga *T. obliquus AS-6-1* by its flocculation property, three cycles of successive adsorption/desorption experiments were conducted in the funnel reactor. Preliminary experiments were conducted to determine the biomass dosage required for complete adsorption of 10 and 30 mg L<sup>-1</sup> Au(III) within 30 min which was found to be at least 0.6 and 1.8 g L<sup>-1</sup>, respectively.

One adsorption/desorption cycle contains adsorption, sedimentation, rinse, sedimentation, desorption, sedimentation and rinse (Fig. 1). All these processes were occurred in one funnel reactor. Biosorption experiments were conducted in triplicates at pH of 2.0 for 30 min under 25 °C. The sedimentation time for microalga separation was 20 min and the sample was collected at a height of one-third from the solution level, and then centrifuged and analysed using Atomic Absorption Spectrometer (AAS Perkin Elmer AAnalyst 400). The concentrated cells were carefully rinsed twice by adding deionized water after adsorption and desorption. The subsequent desorption of bound gold was carried out by adding 50 mL of 0.2 M thiourea at pH of 1.0, 25°C for 15 min. The regenerated microalgae would be used as adsorbents for the next cycle. Each new cycle of adsorption was carried out by supplementing 10 or 30 mg L<sup>-1</sup> of Au(III).

## Results

### Effect of biomass dosage

The results in Table 1 show that the dosage of the two present microalgae  $\geq 0.04$  g L<sup>-1</sup> resulted in approximately 100 % Au(III) adsorption. The algal biomass tested showed a decrease in time required to reach equilibrium with an increase in biomass dosage (Table 1). It took only about 10 to 30 min to reach the maximum uptake at biosorbent dosage from 0.06-0.12 g L<sup>-1</sup> using *T. obliquus AS-6-1*, but more time – up to 90 min at dosage of 0.04 g L<sup>-1</sup>. The time reaching the equilibrium by *T. obliquus* required a little bit longer, with 20 to 40 min at biosorbent dosage from 0.06 - 0.12 g L<sup>-1</sup> and 120 min at dosage of 0.04 g L<sup>-1</sup>. It is worth noting that the adsorption efficiency increased with an increase in biomass dosage but the binding capacity gradually decreased. For the initial Au(III) concentration of 5 mg L<sup>-1</sup>, the maximum adsorption rate achieved by *T. obliquus AS-6-1* was 5.0 mg g<sup>-1</sup> min<sup>-1</sup> within 10 min at biomass dosage of 0.10 g L<sup>-1</sup>, and 2.5 mg g<sup>-1</sup> min<sup>-1</sup> within 20 min at biomass dosage of 0.10 g L<sup>-1</sup> using *T. obliquus* (Fig. 2a).

### **Effect of contact time, pH and temperature**

Almost 100 % of the total Au(III) was quickly adsorbed by 10 mg of dried *T. obliquus* AS-6-1 and *T. obliquus* within 20 min (Fig. 2b). From 30 to 480 min, the two present microalgae retained the constant adsorption capacity of 50 mg g<sup>-1</sup> which indicated the stable equilibrium. The maximum adsorption capacity of 50 mg g<sup>-1</sup> on *T. obliquus* AS-6-1 was found to be at pH 2.0 (Fig. 2c). The uptake slightly decreased to 48.7 mg g<sup>-1</sup> at pH 3.0, and then declined drastically in further increase of pH from 4.0 to 7.0. The maximum adsorption capacity of 50 mg g<sup>-1</sup> on *T. obliquus* was observed at pH 3.0. While at pH of 2.0, it still showed good adsorption potential with Au(III) uptake of 48.87 mg g<sup>-1</sup>. The maximum uptake of 50 mg g<sup>-1</sup> for both of the microalgae was obtained at ambient temperature of 25 °C (Fig. 2d). More than 90 % of Au(III) was effectively adsorbed by *T. obliquus* AS-6-1 and *T. obliquus* from 7 to 60 °C. However, the adsorption capacity was slightly decreased with the further increase in temperature to 60 °C.

### **Effect of initial Au(III) concentration**

An increase was observed in the uptake of *T. obliquus* AS-6-1 with an increasing initial concentration from 5 to 20 mg L<sup>-1</sup>, and no considerable change was observed from an initial concentration of 30 to 50 mg L<sup>-1</sup> (Fig. 2e). The maximum adsorption capacity of *T. obliquus* AS-6-1 was 149.83 mg g<sup>-1</sup> at the initial concentration of 20 mg L<sup>-1</sup>. The adsorption capacity of *T. obliquus* under various Au(III) concentrations showed the similar trend, but the maximum adsorption capacity of 80.77 mg g<sup>-1</sup> obtained at the initial concentration of 10 mg L<sup>-1</sup>. Interestingly, the adsorption efficiency by the tested microalgae decreased with an increase in initial Au(III) concentration.

### **Adsorption isotherm, kinetics and thermodynamics**

The results from the Langmuir model had a higher correlation co-efficient ( $R^2$ ) of 1.00 than the Freundlich model with  $\leq 0.66$  (Table 2). In addition, both  $q_m$  and b value for *T. obliquus* AS-6-1 were higher than those of *T. obliquus*. The maximum adsorption capacity ( $q_m$ ) of *T. obliquus* AS-6-1 was compared to other algal biosorbents from previous studies (Table 3). *T. obliquus* AS-6-1 had a higher  $q_m$  of 181.82 mg g<sup>-1</sup> for

Au(III) as compared to other biosorbents except for the seaweed *Sargassum natans* with a  $q_m$  of 413.7 mg g<sup>-1</sup> (Table 3).

The first order model fit well with only a few data points in the first 20 min and then the experimental data scattered with low correlation coefficient ( $R^2$ ) values for the rest of the period. The Pseudo-second-order model produced a higher  $R^2$  for both the biosorbents tested (Table 4). In addition, there was no pronounced difference between the experimental adsorption capacity ( $q_{e,exp}$ ) and the calculated adsorption capacity ( $q_{e,cal}$ ) at equilibrium for Pseudo-second-order kinetics.

The thermodynamic data obtained from the adsorption of Au(III) ions by the tested microalgae are all negative presented in Table 5.

### **Characterization of biosorbent**

XRF data in Table 6 showed a sharp increase from 0.01 to 9.11 % in Au amount on *T. obliquus* AS-6-1 surface after adsorption. A significant increase in Cl and decrease in Na, Mg, K and Ca concentrations on the algae cell surface were observed after interacted with H<sub>2</sub>AuCl<sub>4</sub>.

FTIR spectra in Fig. 3 indicated the presence of different functional groups in the cell wall of the different biomass. A broadly-stretched intense peak at approximately 3300 cm<sup>-1</sup> was characteristic of hydroxyl groups probably sited on polysaccharide and protein. The absorption peak at around 2920 cm<sup>-1</sup> signified asymmetrical C–H stretching vibration of aliphatic CH<sub>2</sub> group, and the peak at approximately 1643 cm<sup>-1</sup> is indicative of C=O bend for amide probably sited on protein. The broad stretch of C–O–C and C–O at 1000–1200 cm<sup>-1</sup> corresponded to the presence of carbohydrates (Paul et al. 2012; Guo et al. 2013). The same trend was observed in the case of *T. obliquus*. Especially, the intensity at 3281 cm<sup>-1</sup> and bands ranged from 1632 to 1643 cm<sup>-1</sup> had a drastically decrease.

The flocculation efficiency of *T. obliquus* AS-6-1 was much higher than *T. obliquus*, achieved almost 80 % within 20 min but 30 % for the latter (Fig. 5). There was not significant increase in flocculation efficiency after 20 min. Therefore, the sedimentation

time for subsequent experiments on adsorption/desorption cycles was selected as 20 min.

### **Biosorbent regeneration**

The Au(III) adsorption by *T. obliquus* AS-6-1 in the first two cycles remained high (> 97 %) and decreased to 82.63 % in the 3<sup>rd</sup> cycle at initial concentration of 10 mg L<sup>-1</sup>, Fig. 6a. Desorption efficiency was high at 95.95 % in the 1<sup>st</sup> cycle but reduced to 68.96 % in the 3<sup>rd</sup> cycle. At higher concentration of 30 mg L<sup>-1</sup>, the adsorption remained high in the first two cycles and decreased to 70.88 % in the 3<sup>rd</sup> cycle, but performed better in desorption in the range of 80.58 - 98.63 %, Fig. 6c. The adsorption efficiency for *T. obliquus* remained relatively high in the first two cycles in the range of 82-100 % and decreased to 60-70 % in the 3<sup>rd</sup> cycle at initial Au(III) concentration of 10 and 30 mg L<sup>-1</sup>, Fig. 6b and 6d. Desorption efficiency was generally low in all 3 cycles in the range of 14.28 - 75.89 %.

### **Discussion**

The optimal Au(III) adsorption conditions by the tested microalgae were obtained at 0.1 g L<sup>-1</sup> biomass, pH 2.0, 25 °C for 30 min with an initial concentration of 5 mg L<sup>-1</sup>. The biosorbent dosage and pH of Au(III) solution strongly influenced the extent of biosorption, while the adsorption capacity was not significantly influenced by the temperature in the range of 7 - 60 °C. The adsorption rate (Zhang et al. 2016), defined as the amount of adsorbed metal ions per dry cell weight per minute within a period of time, was introduced to determine the optimum biomass dosage. The short-term adsorption of Au(III) within 10 min by self-flocculating microalga *T. obliquus* AS-6-1 showed its advantage in improving adsorption rate which is desirable for industrial application.

The insufficient available Au(III) to the abundant binding sites on the biosorbents may explain why the adsorption efficiency increased but the binding capacity gradually decreased with an increase in biomass dosage (Table 1), which is also proposed by Das (2010). The decrease in adsorption capacity as the pH increased (Fig. 2c) may be due to the less availability of positively charged ligands on cell wall. This is unfavourable in attraction of negatively charged AuCl<sub>4</sub><sup>-</sup> to the cell surface through electrostatic forces.



The decline in uptake at pH 1.0 may be related to the charge reversal of biosorbent below pH 2.0 (Das 2010).

The adsorption capacity of *T. obliquus AS-6-1* at higher Au(III) concentrations (20 - 50 mg L<sup>-1</sup>) was extremely higher than that observed from *T. obliquus* (Fig.2e), which might result from more vacant binding sites on cell surface of *T. obliquus AS-6-1*. Before reaching the maximum uptake, there was a considerable increase in adsorption capacity, which might be due to the higher availability of metal ions. However, with the further increase in Au(III) concentration, the metal ions are needed to overcome the mass transfer resistance and diffuse to the biomass surface by intra-particle diffusion at a slower rate. This may account for the reduction in the adsorption efficiency by the tested microalgae (Fig.2e).

The fit of the biosorption data to the Langmuir isotherm implied that even at the insufficient binding sites, the adsorbates Au(III) do not interact or compete with each other and are adsorbed by forming a monolayer. Kratochvil and Volesky (1998) stated that a favourable biosorbent should have a low Langmuir constant  $b$  and a high  $q_m$  value but regardless of the recovery rate. Some authors proposed that a higher  $q_m$  and a higher  $b$  imply adsorbents with both a high adsorption and recovery rate at low equilibrium concentration (Birungi and Chirwa 2014). In this study, both  $q_m$  and  $b$  value for *T. obliquus AS-6-1* were higher than those of *T. obliquus*, emerging the better adsorbent for recovery of Au(III). *T. obliquus AS-6-1* showed the highest adsorption capacity except for the seaweed *Sargassum natans*, indicating the high potential of *T. obliquus AS-6-1* as the biosorbent for gold recovery.

The results from Table 4 suggested that the system showed a better fit for Pseudo-second order than the first order. This indicated that the rate-limiting step is a chemical adsorption process between Au(III) and microalgae *T. obliquus AS-6-1* and *T. obliquus*. The negative values of  $\Delta G^\circ$  at all temperatures implied that the adsorption of Au(III) onto the present microalgae was spontaneous in nature (Table 5). This could be due to the adequate metal binding sites available for adsorption. A negative  $\Delta H^\circ$  value confirms the exothermic nature of the Au(III) adsorption process by both microalgae. This may explain why the adsorption capacity decreased with an increase in temperature

as observed in Fig. 2d. A negative  $\Delta S^\circ$  is an indication of a decrease in randomness at the solid–liquid interface during the adsorption of metal ions, which implies that the adsorption process was energetically stable (Akram et al. 2017).

XRF data in Table 6 confirmed the presence of Au on the adsorbent surface and implied the probable ion exchange between Na, Mg, K, Ca ions on the algal cells and  $H^+$  in acid gold solution. The changes in bands intensity and wavenumber suggest the involvement of those functional groups tested from FTIR spectra in gold binding. The intensity of the peaks at wavenumbers ranged from 3281 to 3300  $cm^{-1}$  and 1632 to 1643  $cm^{-1}$  changed to a lower value after the interaction of *T. obliquus AS-6-1* and *T. obliquus* with gold, which could imply that the hydroxyl groups and C=O bend for amide on polysaccharides and proteins play an important role in Au(III) adsorption by *T. obliquus AS-6-1* and *T. obliquus*.

Guo et al. (2013) suggested that the polysaccharide excreted from the self-flocculating microalga were responsible for cell self-flocculation. Mata et al. (2009) proposed that hydroxyl groups (O-H) abundant in polysaccharides of the algal cell wall participated in gold recovery. The abundant binding sites of hydroxyl groups on polysaccharides excreted from the self-flocculating microalga may explain why *T. obliquus AS-6-1* performed better in gold adsorption than non-flocculating alga *T. obliquus*.

Compared to the non-flocculating microalgae, a significant change in morphology of the flocculating microalgae was observed in Fig. 4a, with many cells aggregated together to form flocs, which consequently facilitated their gravity sedimentation for biomass recovery. This may result in the higher flocculation efficiency of self-flocculating microalgae *T. obliquus AS-6-1* than non-flocculating microalgae *T. obliquus* (Fig. 4b).

In the adsorption/desorption cycles study, most self-flocculating microalga *T. obliquus AS-6-1* could settle down at the bottom by gravity sedimentation within 20 min, while the high turbidity was observed with non-flocculating microalgae *T. obliquus*. Although the regenerated adsorbent *T. obliquus AS-6-1* can retain high efficiency in adsorption in the 2<sup>nd</sup> cycle, the adsorption performance in next cycle was undesirable. The reduction in adsorption and desorption as the number of cycles proceeded may be owing to the

irreversible Au(III) binding property of the adsorbent and the loss in the dry weight of adsorbent after each cycle.

## **Conclusion**

Compared to the non-flocculating microalga, the self-flocculating microalga not only benefits its biomass recovery by bio-flocculation, but also improves its potential for gold recovery from diluted aqueous solution. The processes of adsorption, sedimentation, rinse and desorption in each adsorption/desorption cycle using bio-flocculation could proceed efficiently in one funnel reactor. The tested self-flocculating microalga *T. obliquus AS-6-1* showed good regeneration potential which retained high adsorption efficiency of > 97 % in the first two cycles. However, further studies are still required to improve the flocculating property of alga adsorbent without loss in biomass for lasting more cycles, especially for most common non-flocculating microalgae.

## **Acknowledgements**

The authors would like to thank the Sedibeng Water, South Africa and the Water Utilization and Environmental Engineering Division at the University of Pretoria for financial and logistical support during the study of gold recovery by microalgae, and appreciate the kind help of Professor Xin-Qing Zhao in Shanghai Jiao Tong University and Professor Jo-Shu Chang in National Cheng Kung University, Taiwan for providing the microalgae strains.

## **References**

- Alam MA, Wan C, Zhao XQ, Chen LJ, Chang JS, Bai FW (2015) Enhanced removal of Zn<sup>2+</sup> or Cd<sup>2+</sup> by the flocculating *Chlorella vulgaris* JSC-7. *J Hazard Mater* 289: 38–45.
- Al-Saidi HM (2016) The fast recovery of gold(III) ions from aqueous solutions using raw date pits: kinetic, thermodynamic and equilibrium studies. *J Saudi Chem Soc* 20: 615–624.
- Akram M, Bhatti HN, Iqbal M, Noreen S, Sadaf S (2017) Biocomposite efficiency for Cr(VI) adsorption: kinetic, equilibrium and thermodynamics studies. *J Environ Chem Eng* 5: 400–411.
- Birungi ZS, Chirwa EMN (2014) The kinetics of uptake and recovery of lanthanum using freshwater algae as biosorbents: comparative analysis. *Bioresour Technol* 160: 43–51.

- Castro L, Blázquez ML, Muñoz JA, González F, Ballester A (2013) Biological synthesis of metallic nanoparticles using algae. *IET Nanobiotechnol* 7: 109–116.
- Chen CY, Kao AL, Tsai ZC, Chow TJ, Chang HY, Zhao XQ, Chen PT, Su HY, Chang JS (2016) Expression of type 2 diacylglycerol acyltransferase gene DGTT1 from *Chlamydomonas reinhardtii* enhances lipid production in *Scenedesmus obliquus*. *Biotechnol J* 11: 336–344.
- Darnall DW, Greene B, Henzl MT, Hosea JM, McPherson RA, Sneddon J, Alexander MD (1986) Selective recovery of gold and other metal ions from an algal biomass. *Environ Sci Technol* 20: 206–208.
- Deplanche K, Macaskie LE (2008) Biorecovery of gold by *Escherichia coli* and *Desulfovibrio desulfuricans*. *Biotechnol Bioeng* 99: 1055–1064.
- Das N (2010) Recovery of precious metals through biosorption — A review. *Hydrometallurgy* 103: 180–189.
- Freundlich, HMF (1906) Über die adsorption in losungen. *Z. Phys. Chem. (Leipzig)* 57A: 385–470.
- Guo SL, Zhao XQ, Wan C, Huang ZY, Yang YL, Alam MA, Ho SH, Bai FW, Chang JS (2013) Characterization of flocculating agent from the self-flocculating microalga *Scenedesmus obliquus* AS-6-1 for efficient biomass harvest. *Bioresour Technol* 145: 285–289.
- Gao X, Zhang Y, Zhao Y (2017) Biosorption and reduction of Au(III) to gold nanoparticles by thiourea modified alginate. *Carbohydr Polym* 159: 108–115.
- Ho YS, McKay G (2000). The kinetics of sorption of divalent metal ions onto sphagnummoss peat. *Water Res* 34: 735–742.
- Ju X, Igarashi K, Miyashita S, Inagaki K, Fujii S, Sawada H, Kuwabara T, Minoda A (2016) Effective and selective recovery of gold and palladium ions from metal wastewater using a sulfothermophilic red alga, *Galdieria sulphuraria*. *Bioresour Technol* 211: 759–764.
- Kuyucak N, Volesky B (1989) Accumulation of gold by algal biosorbent. *Biorecovery* 1: 189–204.
- Kratochvil D, Volesky B (1998) Advances in the biosorption of heavy metals. *Trends Biotechnol* 16: 291–300.
- Langmuir I (1918) The adsorption of gases on plane surfaces of glass, mica and platinum. *J Am Chem Soc* 40:1361–1403.
- Lin Z, Wu J, Xue R, Yang Y (2005) Spectroscopic characterization of Au<sup>3+</sup> biosorption by waste biomass of *Saccharomyces cerevisiae*. *Spectrochim Acta A* 61: 761–765.

Mack C, Wilhelmi B, Duncan JR, Burgess JE (2007) Biosorption of precious metals. *Biotechnol Adv.* 25: 264–271.

Moreno-Garrido I (2008) Microalgae immobilization: current techniques and uses. *Bioresource Technol* 99: 3949–3964.

Mata YN, Torres E, Blázquez ML, Ballester A, González F, Munoz JA (2009) Gold(III) biosorption and bioreduction with the brown alga *Fucus vesiculosus*. *J Hazard Mater* 166: 612–618.

Maruyama T, Terashima Y, Takeda S, Okazaki F, Goto M (2014) Selective adsorption and recovery of precious metal ions using protein-rich biomass as efficient adsorbents. *Process Biochem* 49: 850–857.

Nakajima A (2003) Accumulation of gold by microorganisms. *World J Microb Biot* 19: 369–374.

Paul ML, Samuel J, Chandrasekaran N, Mukherjee A (2012) Comparative kinetics, equilibrium, thermodynamic and mechanistic studies on biosorption of hexavalent chromium by live and heat killed biomass of *Acinetobacter junii* VITSUKMW2, an indigenous chromite mine isolate. *Chem Eng J* 187: 104–113.

Romero-Gonzalez ME, Williams CJ, Gardiner PHE, Gurman S, Habesh S (2003) Spectroscopic studies of the biosorption of Gold(III) by dealginated seaweed waste. *Environ Sci Technol* 37: 4163–4169.

Syed S (2012) Recovery of gold from secondary sources—A review. *Hydrometallurgy* 115-116: 30–51.

Shen N, Birungi ZS, Chirwa EMN (2017) Selective biosorption of precious metals by cell-surface engineered microalgae. *Chem Engineer Trans* 61: 25–30.

Umeda H, Sasaki A, Takahashi K, Haga K, Takasaki Y, Shibayama A (2011) Recovery and concentration of precious metals from strong acidic wastewater. *Mater Trans* 52: 1462–1470.

Volesky B (2007) Biosorption and me. *Water Res* 41: 4017–4029.

Zhou W, Ruan R, Wang J (2015) Bio-flocculation of microalgae: status and prospects. *Current Biotechnol* 4: 448–456.

Zhang X, Zhao X, Wan C, Chen B, Bai F (2016) Efficient biosorption of cadmium by the self-flocculating microalga *Scenedesmus obliquus* AS-6-1. *Algal Res* 16: 427–433.

**Table 1** Au(III) adsorption efficiency and capacity at corresponding equilibrium time with increasing biomass dosage

| Biomass dosage<br>(g L <sup>-1</sup> ) | Equilibrium time<br>(min)    |                    | Efficiency<br>(%)            |                    | Capacity<br>(mg g <sup>-1</sup> ) |                    |
|--|------------------------------|--------------------|------------------------------|--------------------|-----------------------------------|--------------------|
|  | <i>T. obliquus</i><br>AS-6-1 | <i>T. obliquus</i> | <i>T. obliquus</i><br>AS-6-1 | <i>T. obliquus</i> | <i>T. obliquus</i><br>AS-6-1      | <i>T. obliquus</i> |
| 0.02                                   | 120                          | 240                | 70.00                        | 92.93              | 175.00                            | 232.33             |
| 0.04                                   | 90                           | 120                | 99.20                        | 99.07              | 124.00                            | 123.83             |
| 0.06                                   | 30                           | 40                 | 99.53                        | 99.80              | 82.94                             | 83.17              |
| 0.08                                   | 20                           | 30                 | 99.73                        | 99.20              | 62.33                             | 62.00              |
| 0.10                                   | 10                           | 20                 | 99.87                        | 99.67              | 49.93                             | 49.83              |
| 0.12                                   | 10                           | 20                 | 99.13                        | 100                | 41.31                             | 41.67              |

**Table 2** Langmuir and Freundlich adsorption isotherms constants (25 °C, pH=2.0, 0.1 g L<sup>-1</sup> biomass dosage)

| Microalgae         | Langmuir constant       |                             |       | Freundlich constant |                             |       |
|--------------------|-------------------------|-----------------------------|-------|---------------------|-----------------------------|-------|
|                    | b (L mg <sup>-1</sup> ) | $q_m$ (mg g <sup>-1</sup> ) | $R^2$ | n                   | $K_f$ (mg g <sup>-1</sup> ) | $R^2$ |
| <i>T. obliquus</i> | 6.88                    | 181.82                      | 1.00  | 7.43                | 122.35                      | 0.59  |
| <i>AS-6-1</i>      |                         |                             |       |                     |                             |       |
| <i>T. obliquus</i> | 4.77                    | 161.29                      | 1.00  | 8.67                | 112.75                      | 0.66  |

**Table 3** Comparison of adsorption capacity of Au(III) using *T. obliquus AS-6-1* with other algal adsorbents in the literature

| Biosorbent                   | $q_m$ (mg g <sup>-1</sup> ) | pH  | Reference                     |
|------------------------------|-----------------------------|-----|-------------------------------|
| <i>Galdieria sulphuraria</i> | 1.79                        | 2.5 | Ju et al. (2016)              |
| <i>Spyrogira insignis</i>    | 19.7                        | 2   | Castro et al. (2013)          |
| <i>Chlorella vulgaris</i>    | 98.5                        | 2.0 | Darnall et al. (1986)         |
| <i>Sargassum natans</i>      | 413.7                       | 2.5 | Kuyucak and Volesky (1989)    |
| <i>Fucus vesiculosus</i>     | 68.95                       | 7.0 | Mata et al. (2009)            |
| Dealginated Seaweed          | 78.8                        | 3.0 | Romero-Gonzalez et al. (2003) |
| <i>S. obliquus AS-6-1</i>    | 181.82                      | 2   | From this study               |



**Table 4** Parameters of Pseudo-second-order kinetic models for tested microalgae

| Initial concentration<br>(mg L <sup>-1</sup> ) | <i>T.obliquus AS-6-1</i> |   |                                   |                                   | <i>T.obliquus</i> |   |                                   |                                   |
|--|--------------------------|---|-----------------------------------|-----------------------------------|-------------------|---|-----------------------------------|-----------------------------------|
|  | $R^2$                    | $k_2$<br>g mg <sup>-1</sup> min <sup>-1</sup> | $q_{e,cal}$<br>mg g <sup>-1</sup> | $q_{e,exp}$<br>mg g <sup>-1</sup> | $R^2$             | $k_2$<br>g mg <sup>-1</sup> min <sup>-1</sup> | $q_{e,cal}$<br>mg g <sup>-1</sup> | $q_{e,exp}$<br>mg g <sup>-1</sup> |
| 10   | 1.00                     | 0.0014  | 102.04                            | 100.00                            | 1.00              | 0.0014  | 102.04                            | 100.00                            |
| 20   | 1.00                     | 0.0007  | 181.82                            | 176.87                            | 1.00              | 0.0002  | 166.67                            | 160.97                            |
| 30   | 1.00                     | 0.0008  | 178.57                            | 178.73                            | 0.98              | 0.0002  | 158.73                            | 155.33                            |
| 40   | 1.00                     | 0.0008  | 178.57                            | 179.13                            | 0.95              | 0.0001  | 153.85                            | 154.17                            |
| 50   | 0.99                     | 0.0005  | 181.82                            | 183.77                            | 0.95              | 0.0002  | 158.73                            | 163.27                            |

**Table 5** Thermodynamic parameters determined at temperature range 7 - 60 °C for *T. obliquus* AS-6-1 and *T. obliquus*.

| Temperature<br>°C | <i>T. obliquus</i> AS-6-1          |                                    |  | <i>T. obliquus</i>                 |                                    |  |
|-------------------|------------------------------------|------------------------------------|--|------------------------------------|------------------------------------|--|
|                   | $\Delta G$<br>kJ mol <sup>-1</sup> | $\Delta H$<br>kJ mol <sup>-1</sup> | $\Delta S$<br>kJ mol <sup>-1</sup> K <sup>-1</sup> | $\Delta G$<br>kJ mol <sup>-1</sup> | $\Delta H$<br>kJ mol <sup>-1</sup> | $\Delta S$<br>kJ mol <sup>-1</sup> K <sup>-1</sup> |
| 7                 | -5.97                              | -29.607                            | -0.085   | -4.60                              | -26.912                            | -0.080   |
| 25                | -4.78                              |                                    |  | -3.87                              |                                    |  |
| 30                | -3.33                              |                                    |  | -2.73                              |                                    |  |
| 40                | -1.50                              |                                    |  | -0.52                              |                                    |  |
| 50                | -3.79                              |                                    |  | -0.88                              |                                    |  |
| 60                | -0.99                              |                                    |  | -1.25                              |                                    |  |

**Table 6** Elemental composition of *T. obliquus AS-6-1* surface before and after interaction with Au(III)

| <i>T. obliquus AS-6-1</i> | wt % |      |      |      |      |      |
|---------------------------|------|------|------|------|------|------|
|                           | Au   | Cl   | Na   | Mg   | K    | Ca   |
| Before adsorption         | 0.01 | 0.19 | 1.36 | 0.45 | 2.86 | 0.98 |
| After adsorption          | 9.11 | 7.48 | 0.37 | 0.08 | 0.19 | 0.10 |

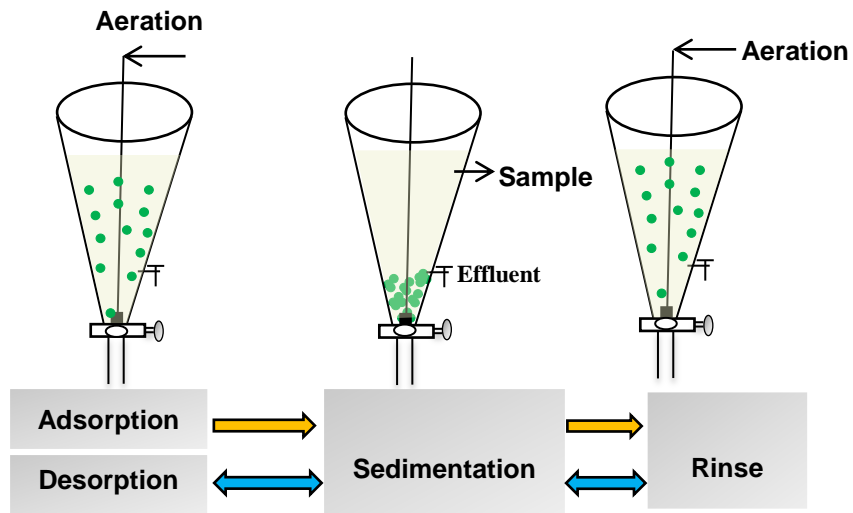


**Fig. 1** Schematic diagram of one adsorption/desorption cycle. The processes of adsorption, sedimentation, rinse and desorption occurred in one funnel reactor. The rinsed microalgae after desorption would be used as adsorbents for the next cycle.

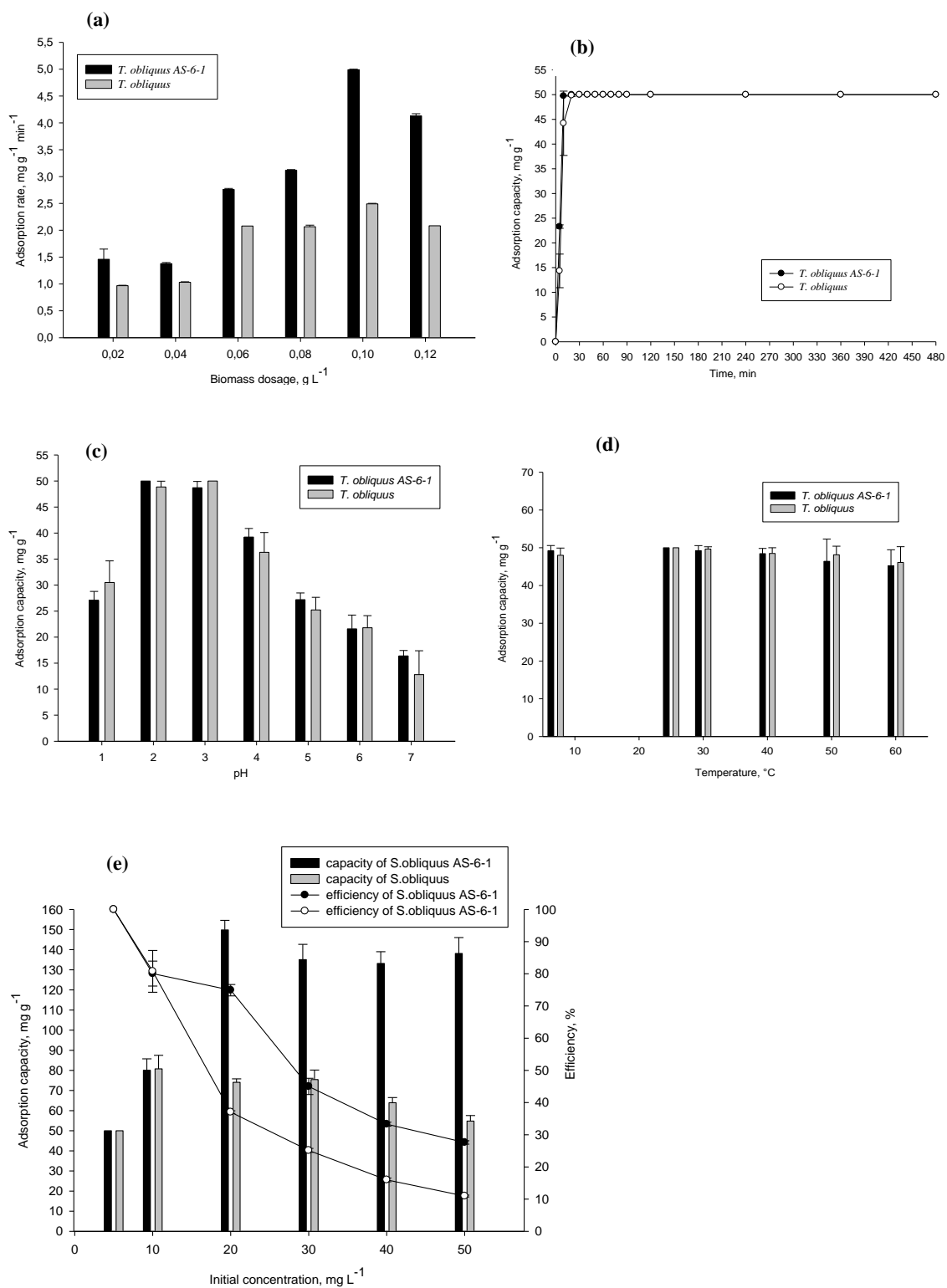


**Fig. 2** Effect of (a) biomass dosage, (b) contact time, (c) pH, (d) temperature, and (e) initial concentration on Au(III) adsorption.

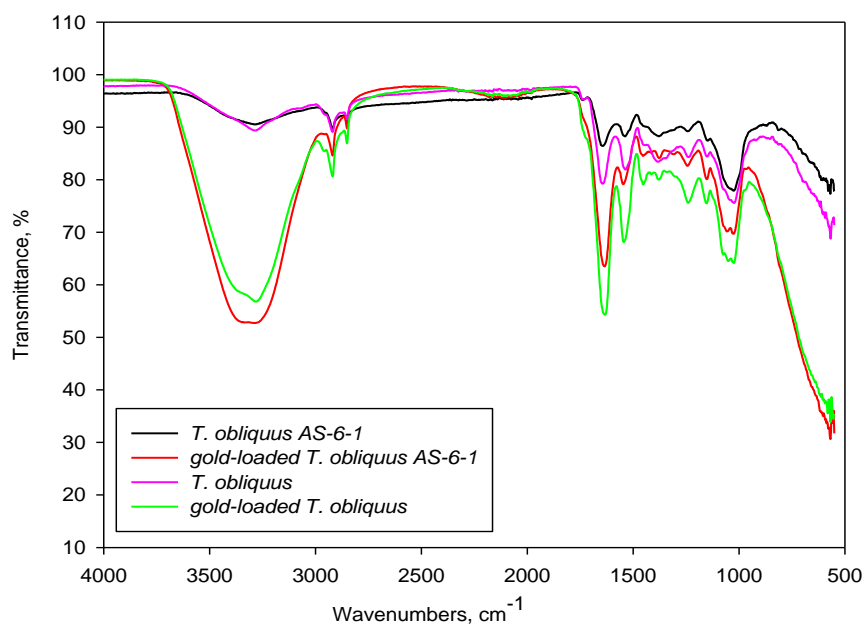


**Fig. 3** FTIR spectra of *T. obliquus* AS-6-1 and *T. obliquus* before and after Au(III) adsorption.

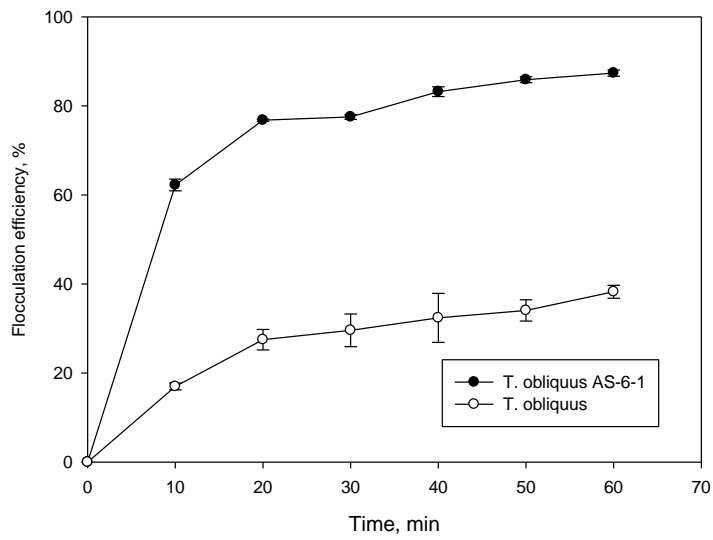
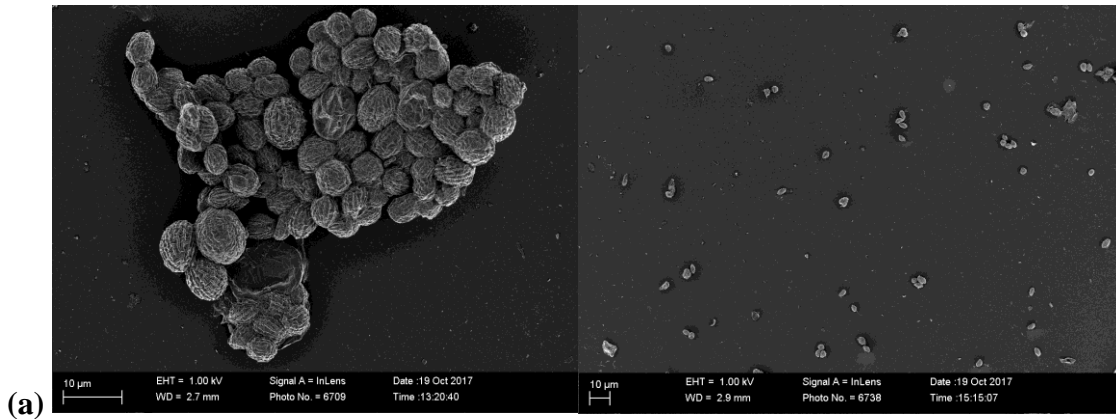


**Fig. 4** (a) SEM images of *T. obliquus* AS-6-1 (left) and *T. obliquus* (right); (b) Flocculation efficiency of tested algae at varying standing time.

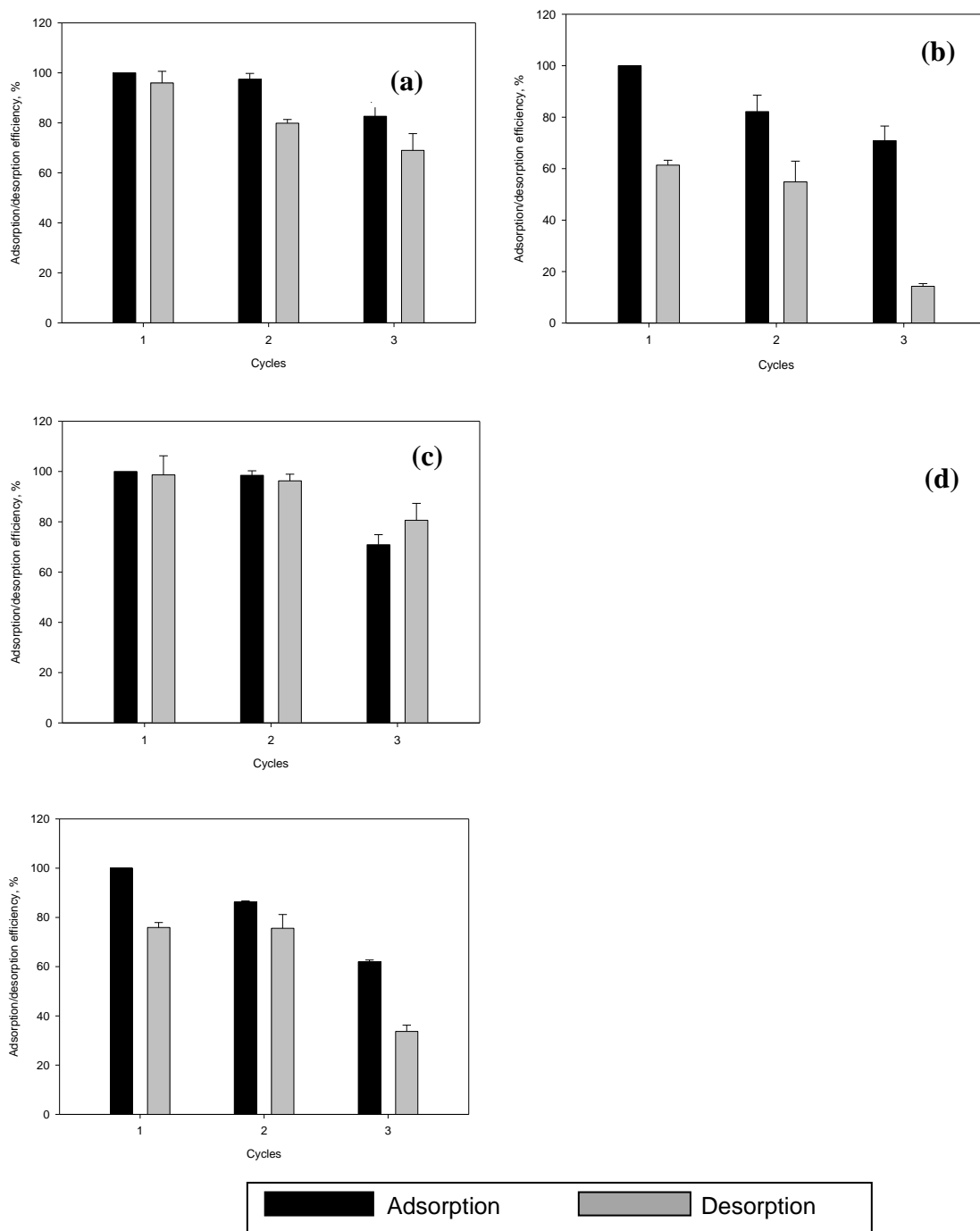


**Fig. 5** Adsorption/desorption efficiency of Au(III) by *T. obliquus* AS-6-1 (a) and *T. obliquus* (b) at initial concentration 10 mg/L; and by *T. obliquus* AS-6-1 (c) and *T. obliquus* (d) at initial concentration 30 mg/L in three cycles.